

The following publication Sun, J., Xue, X., & Cheng, K. W. E. (2020). Four-wheel anti-lock braking system with robust adaptation under complex road conditions. IEEE transactions on vehicular technology, 70(1), 292-302 is available at https://doi.org/10.1109/TVT.2020.3045694

Four-Wheel Anti-Lock Braking System with Robust Adaptation under Complex Road Conditions

J. H. Sun, X. D. Xue, *Senior Member* and K. W. E. Cheng, *Fellow, IEEE*

***Abstract*—The anti-lock braking system(ABS) research based on wheel slip control(WSC) is the classical method and can be found in the literature for almost all automobile braking applications. Despite the significant progress of ABS that has taken place over the last few years, with the recent high demand in autonomous driving, smart control, and electric vehicle, new issues that constitute an open topic for research emerge. Among them, robustness of the braking performance under complex road conditions, the steady-state performance, and reduction of the tracking error are topics of interest that require further study, especially for designing vehicle's four-wheel ABS. This paper aims to propose a four-wheel braking control strategy based on the intelligent FSM-WSC method. The dynamic models under complex braking situations are firstly built including the important issues of the transition of road conditions, the split-road conditions between the left-side wheels and the right-side wheels, even the extreme situation in which road conditions of each wheel are different. To demonstrate control performance, substantial simulation results are analyzed and examined. Finally, performance discussion is presented and it forms a future ABS control and model.**

***Index Terms*—anti-lock braking system(ABS), wheel slip control(WSC), fuzzy sliding mode(FSM), four-wheel ABS, complex road conditions.**

NOMENCLATURE

D	Vehicle stop distance
$\lambda_i, \dot{\lambda}_i$	Real-time longitudinal slip and its dynamics
λ_0	Initial braking λ_i of wheel
$\lambda_{oi}, \lambda_{bi}$	Optimal and best wheel longitudinal slip
$v_{v_x}, \dot{v_{v_x}}$	Vehicle longitudinal velocity and its dynamics
v_0	Initial braking v_{v_x} of vehicle
$\omega_i, \dot{\omega_i}$	Wheel longitudinal angular speed and its dynamics
μ_i	Road friction coefficient of single wheel
F_{air}	Drag force of whole vehicle from air
F_{f_i}	Friction force of single wheel
F_{r_i}	Rolling friction force of single wheel
T_{b_i}	Braking torque of single wheel
t_k	Arbitrary time of instant simpling point
Δt	Operational period of automatic detection module
$a_{\omega_i(t_k)}$	Instant wheel angular acceleration of wheel
$a_{\omega_m(i)}$	Average of wheel angular acceleration
$a_{\omega_m(r)}$	Reference value of $a_{\omega_{m(i)}}$ for variety of roads
$d_{\omega_F(t_k)}$	ω_i differential for the front wheels at instant time
$d_{\omega_R(t_k)}$	ω_i differential for the rear wheels at instant time
$d_{\omega_F(r)}$	Reference value of $d_{\omega_F(k)}$
$d_{\omega_R(r)}$	Reference value of $d_{\omega_R(k)}$
β_i	Force weight of single wheel
$e_i, \dot{e}_i$	Error between λ_{oi} and λ_i and its dynamics
$K_{(P,I,D)_i}$	Output variable of the PID part
$F_{(p,i,d)_i}(e_i, \dot{e}_i)$	Weighting value of $K_{(P,I,D)_i}$
$k_{(p,i,d)_0}$	Initial variable of the PID part
$u_i(t)$	Control object of ABS controller
$I_i(t)$	Uncertain interference of braking system
$S_i(t), \dot{S}_i(t)$	Adaptive sliding surface and its dynamics
$\varepsilon_i(t)$	Compensation of the $I_i(t)$

I. INTRODUCTION

THE ABS is a very attractive research topic for ground vehicles since it has the capability to keep the wheel from locking during the vehicle braking period, i.e., the wheel steering remains controllable until the vehicle stops. In recent years, thanks to technological advances in in-wheel technology(IWT), the WSC method has been proposed and studied as a promising alternative for establishing the ABS of automobile [1], [2]. In particular, modern electric and automated vehicles require the ABS controller with high robustness and stability, and therefore, several strategies have been proposed to perfect the WSC method and applied to a quarter vehicle model. For an instant, the fuzzy sliding mode(FSM) control, which optimizes the control performance of ABS controller by adapting the sliding surface that describes the desired system behavior, is widely used and considered as the most popular and important strategy. Originally, the ABS based on the switching control logic threshold method was introduced in the process of automobile braking industry [3], but a few innovative and early papers [4], [5] proposed its drawbacks of both robust performance and control accuracy as it depends on the selecting of control thresholds, which need further experimental insight. Besides, in most cases, industrial processes of the WSC based ABS in the ground vehicles use rule-based multiphase modulation of the wheel torque through the hydraulic brake actuators [6], whereas this kind of hydraulic brake actuator occupied large area is considered as a basic execution unit of the traditional ABS. Despite the fact that the hydraulic brake actuator is widely used in the automobile industry, the latest trends in automotive electrification and automation generate some new challenges [7] about the optimization of WSC based ABS that can be summarized below.

Although the electric vehicle(EV) considered as the energy saving and environmental friendly representative stands out in a variety of ground vehicles and becomes more and more popular in the world, there are not, as of yet, existing EVs provide the pure electric ABS inside its control system. If the existing EVs still use the hydraulic ABS, they must make corresponding sacrifices, e.g., reserving enough space to install the brake tank, adding some mutual conversion steps of electrical and non-electrical signals [8], [9]. For this reason, many kinds of research are focused on the electro-hydraulic (EHB) brakes, as the strict legislative regulations and functional limitations for mass-production vehicles still require the joint operation of electric motors and traditional chassis systems, some of them have been successfully implemented in the lab for a variety of EVs. For instance, Castillo et al. proposed a novel EHB with the tire-road friction estimation and continuous brake pressure control mainly based on a fuzzy logic control scheme and Kalman-filter-based estimation algorithm and incorporated a hydraulic pump, in paper [5]. Throughout this paper, the proposed EHB ABS with more accurate and fast pressure control was verified with shorter braking distances and higher deceleration rates compared with the traditional hydraulic ABS. The advanced control function of decoupled EHB brake system, to deal with the continuous wheel slip control with variation of the brake pedal feel and brake judder compensation, was mentioned in paper [10] by Savitski et al.. It has been verified with many advantages, such as, reducing braking distances, improving the robust performance and avoiding the control effects that overlap in different operational modes. Furthermore, Tavernini et al. presented an explicit nonlinear model predictive ABS controller for electro-hydraulic braking systems in paper [11], which shows that the electric motors have the capability to provide a fast dynamic response and more accurate to track λ_o. However, the ABS based on EHB technology still requires the undesired hydraulic pump, which hinders the further development of EV, as EHB inevitably experience delays. In particular, all electronic applications inside an EV require control responses in the order of tens to hundreds of milliseconds to work properly. Consequently, further research and development efforts are still necessary in order to yield the pure-electric ABS and bring this technology to the industrial and commercial level.

Another problem is the modern and coming generations of electric and automated vehicles require high robustness and high stability, especially for emergency braking situations. To date, a plethora of control strategies have been proposed to tackle this difficulty. These control algorithms range from linear method, such as proportional-integral-derivative (PID) control [12] to fuzzy logic control [9], and from nonlinear method to sliding mode [13]–[15]. To yield a more suitable control scheme with enough robust and adaptive performance, most of the known studies in vehicle braking incorporate a variety of control algorithms, among which the most common strategies are fuzzy control and sliding mode control [3], [6], [16], [17], etc. For example, Savitski described an adaptive continuous WSC developed for the decoupled brake system, whose control strategy was constructed of proportional-integral (PI), sliding-mode PI and integral-sliding-mode [3]. Furthermore, this paper verifies that this proposed control strategy has substantial adaptability and robust performance through road experiments on low-μ and high-μ surfaces. Unlike other papers, Han show us the development of the ABS applied in an EV without λ_i and μ_i information in [6], which is verified as a cost-competitive method to achieve anti-lock requirements during the vehicle braking, as it only uses sensors that are measurable in production vehicles. In addition, a novel two-time-scale redesign ABS controller is mentioned by Sun et al. in paper [17], which is simple without considering the road condition curve. Although this two-time-scale technology is not suitable for real vehicle braking control, this control idea is a heuristic method for the advancement of braking technology. Even though some existing control approaches are reasonably effective, several challenges have not been fully addressed yet, e.g., the pure electric ABS without using hydraulic pump, more complexed braking road conditions and higher requirements of robust control performances [18], [19].

This paper presents a four-wheel ABS based on the fuzzy sliding mode wheel slip control scheme (FSM-WSC), which is verified as a particularly promising candidate to satisfy the requirements of nowadays ABS controller. The organization of this paper is as follows: Section II shows the operational basis of WSC based ABS, such as the vehicle dynamics and the wheel slip characteristics. After that, the four-wheel ABS model is established. Unlike the instantaneous split-friction surface method [20], the intelligent detection module is described in Section III, which is constructed of the automatic detection of road condition and the wheel smooth-braking adjustment. Section IV shows the design process in detail, and the control object and control steps are all included. In Section V, attention is paid to the simulation and results in discussion, which mainly focuses on dealing with complex road conditions, to verify the control performance of this proposed four-wheel ABS with FSM-WSC based ABS controller. Finally, Section VI concludes this paper.

II. Fundamental of WSC based ABS

Parameters of the proposed four-wheel ABS are shown in Table I, unless otherwise noted, $(i = 1, 2, 3, 4)$ represent the front-left(FL), front-right(FR), rear-left(RL) and rear-right(RR) wheels, respectively.

TABLE I
PARAMETERS OF FOUR-WHEEL ABS BASED ON BYD F0.

Sign	Parameter	Value
μ_{r_i}	Rolling friction coefficient	0.015
$M(kg)$	Full mass of vehicle	938
$R_w(m)$	Single wheel radius	0.2768
$m_w(kg)$	Mass of single wheel	12
$J(kg/m^2)$	Inertia of single wheel	0.92
$\rho(kg/m^3)$	Air density	1.25
C_{air}	Air resistance coefficient	0.23
$A_{air}(m^2)$	Air resistance area	2.37

The single wheel vehicle dynamics is well-established and widespread used [21], which mainly focused on designing a suitable controller and generating λ_o on different roads. This paper aims to redesign a more realistic vehicle dynamics model that can satisfy the modern ABS requirements and suitable for four-wheel ABS. In general, the two main operational fundamentals: the vehicle dynamics and the wheel slip characteristic, are required to be analyzed before the establishment of the ABS.

A. Dynamical analyses of Vehicle

The dynamic characteristics: the single wheel and the whole vehicle are formulated in (1), respectively. In the real-time implementation, there are some forces that provide little effect overall the control process, whereas affect the instant condition during some transient segments. For example, the effect of F_{air} is necessary as v_{v_x} is one of its construct components, and F_{r_i} affects $\dot{v_{v_x}}$ as long as the vehicle is in a rolling state. Therefore, these forces are explicitly bound to consider it for the establishment of the dynamical vehicle model.

$$\begin{cases} \dfrac{d\omega_i}{dt} = \mathbf{A} = \dfrac{R_w}{J}\mathbf{F_f} - \dfrac{1}{J}\mathbf{T} \\ \dfrac{dv_{v_x}}{dt} = \dot{v}_{v_x} = -\dfrac{1}{M}[\mathbf{F_f}^{\mathsf{T}}\mathbf{I} + \mathbf{F_r}^{\mathsf{T}}(\mathbf{I} - \mathbf{S_1}) + F_{air}] \end{cases} \tag{1}$$

Here, $\mathbf{A}$ is a matrix of $\dot{\omega}_i$, $\mathbf{S_1}$ and $\mathbf{T}$ are constructed by instant wheel data, describe λ_i and T_{b_i}, respectively.

$$\mathbf{A} = \begin{bmatrix} \dot{\omega}_i \end{bmatrix}, \quad \mathbf{S_1} = \begin{bmatrix} \lambda_i \end{bmatrix}, \quad \mathbf{T} = \begin{bmatrix} T_{b_i} \end{bmatrix} \tag{2}$$

Besides, $\mathbf{F_f}$ and $\mathbf{F_r}$ represent F_{f_i} and F_{r_i}, encompassing the real-time data at each sampling time for every single wheel (FL, FR, RL and RR), respectively.

$$\mathbf{I} = \begin{bmatrix} 1 \end{bmatrix}, \quad \mathbf{F_f} = \begin{bmatrix} F_{f_i} \end{bmatrix}, \quad \mathbf{F_r} = \begin{bmatrix} F_{r_i} \end{bmatrix} \tag{3}$$

Finally, the description of the aforementioned forces are summarized and shown in (4).

$$\begin{cases} F_{f_i} = \dfrac{\mu_i \cdot M \cdot g}{\beta_i} \\ F_{r_i} = \dfrac{\mu_{r_i} \cdot M \cdot g}{\beta_i} \\ J = m_w \cdot R_w^2 \\ F_{air} = (0.5 \times \rho \cdot C_{air} \cdot A_{air} \cdot {v_{v_x}}^2) \end{cases} \tag{4}$$

B. Characteristic Analyses of Wheel Slip

In recent years, a variety of ABS controllers found in the literature for most applications are designed based on the popular magic formula known as the tire-road interaction(TRI) and firstly proposed by Pacejka [22], [23]. The sundry tire-road friction model is considered, and the relationship between λ_i and μ_i of the road is shown in Fig. 1 intuitively.

As λ_i is used to describe the relationship between v_{v_x} and ω_i, to illustrate the characteristics of λ_i at every sampling time, the extra variable $\dot{\lambda}_i$ is defined, which can be obtained by calculating the time derivatives of λ_i. These variables related to λ_i and used in WSC function can be expressed as (5).

$$\begin{cases} \lambda_i = \dfrac{v_{v_x} - \omega_i R_w}{v_{v_x}} \\ \dfrac{d\lambda_i}{dt} = \dot{\lambda}_i = -\dfrac{\dot{\omega}_i R_w - \dot{v}_{v_x}(1 - \lambda_i)}{v_{v_x}} \end{cases} \tag{5}$$

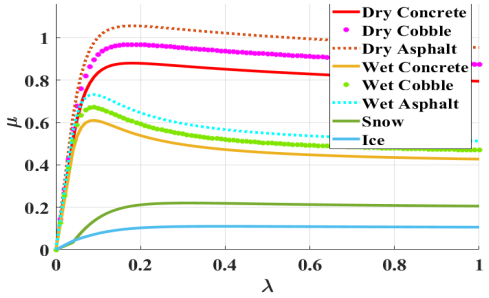

Fig. 1. Relationships between λ_i and μ_i.

In general, each single wheel has its own characteristics $(\lambda_i, \dot{\lambda}_i)$ during the whole braking period, that is to say, four different instant situations are required. Using matrix $\mathbf{S_2}$ to represent the $\dot{\lambda}_i$ characteristics, the above (5) can be modified and summarized in (6), after incorporating with (1). Measurements of ω_i are imported to the λ_i characteristics, based on previous dynamical analyses of vehicle, all possible variables of λ_i characteristics are demonstrated as below:

$$\begin{cases} \mathbf{S_1} = \mathbf{I} - \dfrac{R_w}{v_{v_x}}\mathbf{W} \\ \mathbf{S_2} = -\dfrac{R_w}{v_{v_x}}\mathbf{A} + \dfrac{\dot{v}_{v_x}}{v_{v_x}}(\mathbf{I} - \mathbf{S_1}) \end{cases} \tag{6}$$

Here, $\mathbf{W}$ represents ω_i at each sampling time which obtained from the in-wheel angular speed sensors(IWASS).

$$\mathbf{W} = \begin{bmatrix} \omega_i \end{bmatrix}, \qquad \mathbf{S_2} = \begin{bmatrix} \dot{\lambda}_i \end{bmatrix} \tag{7}$$

III. Intelligent Detection Module of FSM-WSC

Although it is not easy to define a suitable reference factor that based on the desired system behavior, the accuracy of the dynamical model establishment can dramatically decrease the effect derived from the differential between the optimal reference factor and the real one. Therefore, the above analyses of vehicle dynamics provide a good guarantee for the following design module. Assuming that the vehicle is driving on a horizontal road with a straight-line situation, unless otherwise noted, all the following analyses and simulations are considered under this case. The block diagram shown in Fig. 2 illustrates the control method of proposed FSM-WSC based four-wheel ABS. It can be seen from Fig. 2 that the proposed control method includes two modules. One of which is the automatic detection module of road condition and the other is the smooth-braking adjustment module.

A. Automatic Detection Module of Road condition

For every single wheel, IWASS fixed inside the wheel. Besides, as mentioned in (5) and (6), $\dot{\omega}_i$ is related to μ_{r_i} and λ_i. After multiple braking training, the earliest time that the vehicle braking performance reaches steady state, which is also defined as Δt, is selected. During this period, $a_{\omega_i(t_k)}$ can also be calculated: $\dot{\omega}_i = f(\mu_{r_i}, \lambda_i)$, where the sampling frequency is defined as $1kHz$.

$$a_{\omega_{m(i)}} = \frac{a_{\omega_i(t_0)} + \cdots + a_{\omega_i(t_k)} + \cdots + a_{\omega_i(t_{\Delta t})}}{n} \tag{8}$$

Then $a_{\omega_{m(i)}}$ can be calculated based on (8), where, n is set as the number of sampling time calculated as: $\frac{t_{\Delta t} - t_0}{1kHz} + 1$.

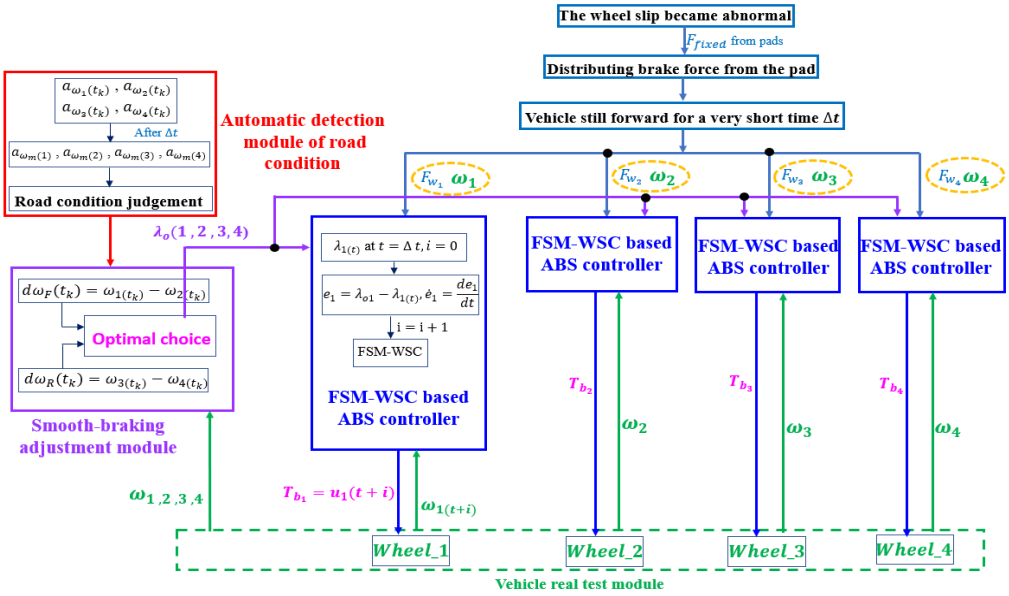

Fig. 2. Control structure of proposed intelligent detection module.

Therefore, the judgment rules for road condition can be summarized as below,

1) $0 < a_{\omega_m(i)} \leq a_{\omega_m(r)}$(Dry Asphalt),
output parameters of the road: ($\mu_i = \mu_{D3}$, $\lambda_{bi} = \lambda_{D3}$).
2) $a_{\omega_m(r)}$(Dry Asphalt) $< a_{\omega_m(i)} \leq a_{\omega_m(r)}$(Dry Cobble),
output parameters of the road: ($\mu_i = \mu_{D2}$, $\lambda_{bi} = \lambda_{D2}$).
3) $a_{\omega_m(r)}$(Dry Cobble) $< a_{\omega_m(i)} \leq a_{\omega_m(r)}$(Dry Concrete),
output parameters of the road: ($\mu_i = \mu_{D1}$, $\lambda_{bi} = \lambda_{D1}$).
4) $a_{\omega_m(r)}$(Dry Concrete)$< a_{\omega_m(i)} \leq a_{\omega_m(r)}$(Wet Asphalt),
output parameters of the road: ($\mu_i = \mu_{W3}$, $\lambda_{bi} = \lambda_{W3}$).
5) $a_{\omega_m(r)}$(Wet Asphalt)$< a_{\omega_m(i)} \leq a_{\omega_m(r)}$(Wet Cobble),
output parameters of the road: ($\mu_i = \mu_{W2}$, $\lambda_{bi} = \lambda_{W2}$).
6) $a_{\omega_m(r)}$(Wet Cobble)$< a_{\omega_m(i)} \leq a_{\omega_m(r)}$(Wet Concrete),
output parameters of the road: ($\mu_i = \mu_{W1}$, $\lambda_{bi} = \lambda_{W1}$).
7) $a_{\omega_m(r)}$(Wet Concrete)$< a_{\omega_m(i)} \leq a_{\omega_m(r)}$(Snow),
output parameters of the road: ($\mu_i = \mu_S$, $\lambda_{bi} = \lambda_S$).
8) When $a_{\omega_m(r)}$(Snow)$< a_{\omega_m(i)} \leq a_{\omega_m(r)}$(Ice),
output parameters of the road: ($\mu_i = \mu_I$, $\lambda_{bi} = \lambda_I$).

B. Smooth-braking adjustment module

In general, the FSM-WSC based ABS controller starts to work after the road condition automatic detection module provided the road condition parameters (μ_{road}, λ_{best}, road condition), especially for single wheel braking control module. However, the road condition parameters of each wheel have considerable variation if the road conditions of the left-side wheels are different from the ones of the right-side wheels. This situation will degrade the drive safety and the braking performance and hence could result in the hidden safety hazard, such as the rollover. To deal with this tricky problem, the smooth-braking adjustment module is proposed in this paper. The control strategy of the proposed smooth-braking adjustment is to provide a trade-off between the safety and the short stopping distance during the whole ABS control period, shown as Fig. 2. Besides, (9) demonstrates the calculation method of $d_{\omega_F(t_k)}$ and $d_{\omega_R(t_k)}$.

$$\begin{cases} d_{\omega_F(t_k)} = \omega_{1(t_k)} - \omega_{2(t_k)} \\ d_{\omega_R(t_k)} = \omega_{3(t_k)} - \omega_{4(t_k)} \end{cases} \tag{9}$$

The main control strategy is to select λ_o for the left and right wheels, which ensures $d_{\omega_F(t_k)}$ and $d_{\omega_R(t_k)}$ satisfy the safety requirements during braking period, where $d_{\omega_F(r)}$ and $d_{\omega_R(r)}$ are selected based on the safety braking requirement.

$$|d_{\omega_F(t_k)}| < d_{\omega_F(r)}, \quad |d_{\omega_R(t_k)}| < d_{\omega_R(r)} \tag{10}$$

This λ_o for each single wheel can achieve the shortest distance brake based on smooth braking.

$$\begin{cases} \lambda_{o(1,2)} = f(\mu_{(1,2)}, \lambda_{b(1,2)}, d_{\omega_F(t_k)}, d_{\omega_F(r)}, v_{v_x}, \omega_{(1,2)}) \\ \lambda_{o(3,4)} = f(\mu_{(3,4)}, \lambda_{b(3,4)}, d_{\omega_R(t_k)}, d_{\omega_R(r)}, v_{v_x}, \omega_{(3,4)}) \end{cases} \tag{11}$$

IV. Design of FSM-WSC Based on ABS Controller

Then the vehicle starts to brake under the control of the proposed FSM-WSC based ABS controller. This section shows the design details of this ABS controller, which is also illustrated in Fig. 2, inside the blue area. The main control algorithm of this sliding mode wheel slip controller is repeated for each sampling time and can be performed.

A. Wheel Slip Function

As mentioned above, the output variable of the ABS controller is T_{b_i}, which is used to adjust ω_i for maintaining λ_i at the reference value. The variation in $\dot{\lambda}_i$ can be expressed more intuitively below by incorporating (1) into (6). As a result, the evolutionary form of T_{b_i}, which is also considered as the control variable of the ABS controller module, can be modified and expressed in (13), since ($\mu_i >> \mu_{r_i}(1-\lambda_i)$).

$$\dot{\lambda}_i = -\frac{1}{v_{v_x}}([\mu_i g + \mu_{r_i} g(1-\lambda_i)](1-\lambda_i)) + \frac{T_{b_i}}{v_{v_x} m_w R_w} \tag{12}$$

$$bT_{b_i} = \dot{\lambda}_i + \frac{1}{v_{v_x}}[\frac{F_{f_i}\beta_i(1-\lambda_i)}{M} + \frac{F_{r_i}(1-\lambda_i)}{m_w} + \frac{F_{air}(1-\lambda_i)}{M}] \tag{13}$$

Consequently,

$$\begin{cases} f(\lambda_i) = \dfrac{1}{v_{v_x}}[F_{f_i}(\dfrac{1}{m_w} + \dfrac{\beta_i(1-\lambda_i)}{M}) + \dfrac{F_{air}(1-\lambda_i)}{M}] \\ T_{b_i} = \dfrac{\dot{\lambda}_i + f(\lambda_i)}{b} \\ b = \dfrac{1}{v_{v_x} m_w R_w} \end{cases} \tag{14}$$

B. Fuzzy PID Part of FSM-WSC Based ABS Controller

To design the ABS controller, define $e_i = \lambda_{oi} - \lambda_i$ to track the error between λ_o generated by the wheel smooth-braking adjustment module and λ_i. Thus the time derivatives of this error, is expressed as $\dot{e}_i = \frac{de_i}{dt} = \dot{\lambda}_{oi} - \dot{\lambda}_i$. The wheel slip tracking error characteristics $(e_i, \dot{e}_i)$ in the continuous-time domain are given in (15), in a four-wheel mode.

$$(e_i, \dot{e}_i) = (\lambda_{oi} - (1 - \frac{R_w\omega_i}{v_{v_x}}), \frac{d\lambda_{oi}}{dt} - (bT_{b_i} - f(\lambda_i))) \tag{15}$$

$(e_i, \dot{e}_i)$ are used as the fuzzy controller's input variables to regulate F_{p_i}, F_{i_i} and F_{d_i} in a robust way based on fuzzy-rules. Finally, K_{P_i}, K_{I_i} and K_{D_i} are obtained and expressed below.

$$K_{(P,I,D)_i} = F_{p_i}(e_i, \dot{e}_i) \times k_{p_0} \tag{16}$$

C. Sliding Mode Part of FSM-WSC Based ABS Controller

Generally, the ABS controller with the above fuzzy PID control strategy has the capability to mitigate the effect generated by uncertain disturbances, whereas its robustness still not enough if there are complicated road conditions and/or uncertain disturbances, especially in controlling response speed and remaining in the stability zone. For this reason, the sliding mode control scheme is added, assume that the system with $I_i(t)$, $\dot{\lambda}_i$ can be described as: $\dot{\lambda}_i = f(\lambda_i) + b(u_i(t) + I_i(t))$. Based on (13) and (14), the control object is derived,

$$u_i(t) = \frac{\dot{\lambda}_i - f(\lambda_i)}{b} - I_i(t) \tag{17}$$

The design of the sliding mode function to serve as an internal sliding control module for the ABS controller is of fundamental importance, as it is used to decide whether the control object in an optimal adaptive area. Using $(S_i, \dot{S}_i)$ to denote this sliding mode function, shown in (18).

$$\begin{cases} S_i = e_i + K_{P_i}\displaystyle\int e_i dt + K_{I_i}\int\int e_i d^2t + K_{D_i}e_i \\ \dfrac{dS_i}{dt} = \dot{S}_i = \dot{e}_i + K_{P_i}e_i + K_{I_i}\displaystyle\int e_i dt + K_{D_i}\dot{e}_i \end{cases} \tag{18}$$

Lyapunov stability function $V = \frac{1}{2}S^2, \dot{V} < 0$ is used to propose the S design for the sliding mode control strategy that allows the system with the desired performance while ensuring the stability of the ABS braking controller. As a result, the dynamics of the defined sliding surface can be expressed in another way: $\dot{S}_i = -\varepsilon_i(t)sign(S_i) - I_i(t)$, after combining the exponential approach law. Besides, $I_i(t)$ can be largely eliminated, shown as (19)

$$S_i\dot{S}_i = -\varepsilon_i(t)|S_i| - I_i(t)S_i < 0 \Longrightarrow \varepsilon_i(t) > |I_i(t)| \tag{19}$$

Here, $\varepsilon_i(t)$ is used to judge whether the sliding mode existence condition is satisfied. Using the integral method to estimate the upper bound of $\varepsilon_i(t)$, then $\hat{\varepsilon}_i(t) = \eta\int_0^t \Delta\varepsilon_i dt$. Finally, the control object can be obtained,

$$u_i(t) = \frac{\dot{\lambda}_i - f(\lambda_i)}{b} + \dot{S}_i + \hat{\varepsilon}_i(t)sign(S_i) \tag{20}$$

The fuzzy rule of sliding mode is proposed: when $S_i\dot{S}_i > 0$, $\hat{\varepsilon}_i(t)$ needs to be increased; when $S_i\dot{S}_i < 0$, $\hat{\varepsilon}_i(t)$ needs to be decreased.

V. Simulation and Results

The control performances of the proposed FSM-WSC based ABS controller has advantages compared with the pure PID based ABS controller and fuzzy PID based ABS controller [24]. Besides, this type ABS controller is illustrated with enough robust and adaptive capability to overcome the negative impact generated by abrupt changes in TRI and vehicle model parameters, e.g., the road condition disturbances: $\mu_i(\lambda_i)$ curve shifting and the vehicle parameters disturbances: vehicle mass. However, [24] only considers the single-wheel braking situation, which is not sufficient to be directly applied to the actual vehicle. Unless otherwise noted, $v_0 = 100km/h$ is selected to show simulation results.

A. Initial conditions for vehicle braking

The reasonable assumptions based on actual braking conditions of vehicle are given: vehicle is driven under the straight-line case; $\lambda_0(t = 0s) = 0.6$ and $v_0 = 100$ km/h; F_{r_i} and F_{air} are all considered; T_{b_i} is a constant, during $\Delta t = 0.009s$; $d_{\omega_F(r)}$ and $d_{\omega_R(r)}$ are selected equal to $6(rad/s)$.

As $a_{\omega_{m(i)}}$ for different roads are required, its change under different road conditions after training are given and shown in Figure 3. The road conditions considered in this vehicle braking simulation are dry, wet, snow, and ice roads, moreover, for the most common dry road and wet road, both are further divided into concrete, cobble and asphalt types.

B. Braking results for the transition of road conditions

For the real vehicle braking case, the road condition does not always keep unchanged during braking, the common situations are that there are multi-segment road surfaces during braking. To better illustrate the control performance of this proposed ABS controller, the simulation results that the vehicle braking on the transition of road conditions are given. For most braking situations, which from dry road to wet road, from dry road to snow road and from wet road to snow road often exist. The braking performances of four wheels are similar. Thus, the braking performance of the left-front wheel will be illustrated and discussed. For the results given in this subsection, the braking operation is assumed as,

1) $0 \le t \le 0.009s$, the intelligent detection module operates.
2) $0.009 < t \le 1.5s$, the vehicle brakes under the control of ABS controller until the transition of road conditions.

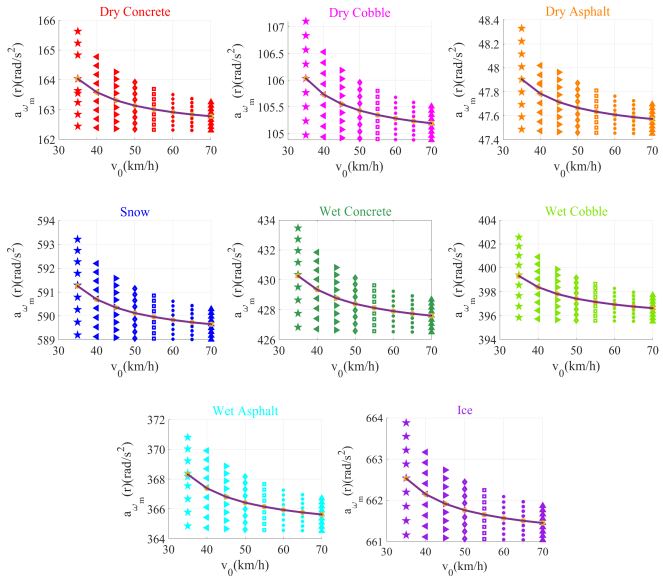

Fig. 3. $a_{\omega_m(i)}$ of different roads

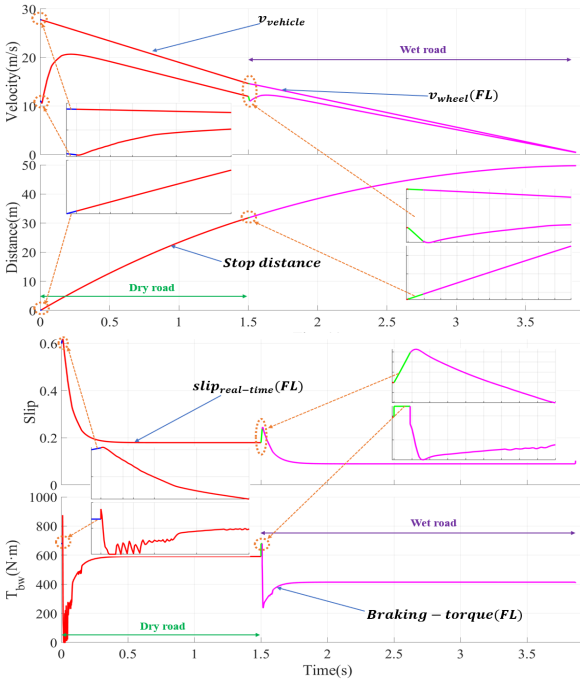

Fig. 4. The transition of road conditions: dry road to wet road.

3) $1.5s < t \leq 1.59s$, the intelligent detection module restarts to work and offers the updated road condition.
4) $1.5 < t \leq t_{stop}$, ABS controller works.

Figure 4 illustrates the braking details, with the transition of road conditions: dry to wet roads,where v_{v_x}, D, and the real-time regulating details of λ_i, T_{bi} are given. At first, $\lambda_0 = 0.6$ is set, then decreases to achieve λ_{o1} given by the intelligent automatic detection module, accompanying by T_{b_i} to adjust ω_i. When the road condition is suddenly changed, λ_i becomes abnormal and touches off a new round of the road condition automatic detection mechanism. Consequently, the ABS controller receives the updated road signal and starts to operate.

Similar to the transition of road conditions described in Figure 4, two other cases are also studied and shown in

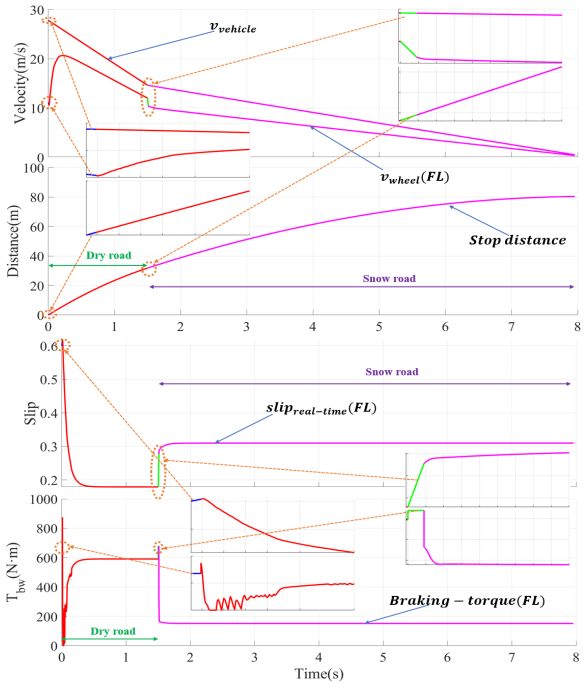

Fig. 5. The transition of road conditions: dry road to snow road.

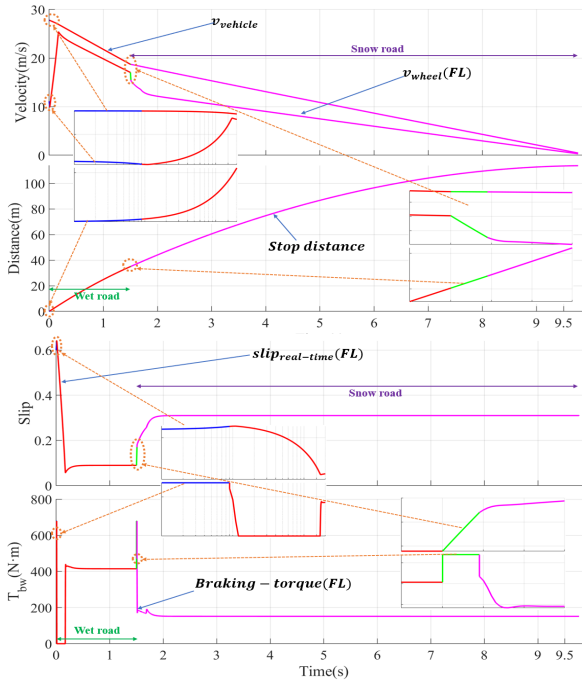

Fig. 6. The transition of road conditions: wet road to snow road.

Figure 5 and Figure 6, respectively. The regulation details of ω_i, λ_i and T_{b_i} are shown in these figures.

C. Results of four-wheel ABS

Another complex case is the split-road conditions, in which wheels on the same side have the same road condition. Based on characteristic analyses mentioned in above, the wheel smooth-braking adjustment part is added into the intelligent detection module of this ABS controller to eliminate the probability of rollover caused by a large deviation of ω_i between the left wheel and right wheel during vehicle braking.

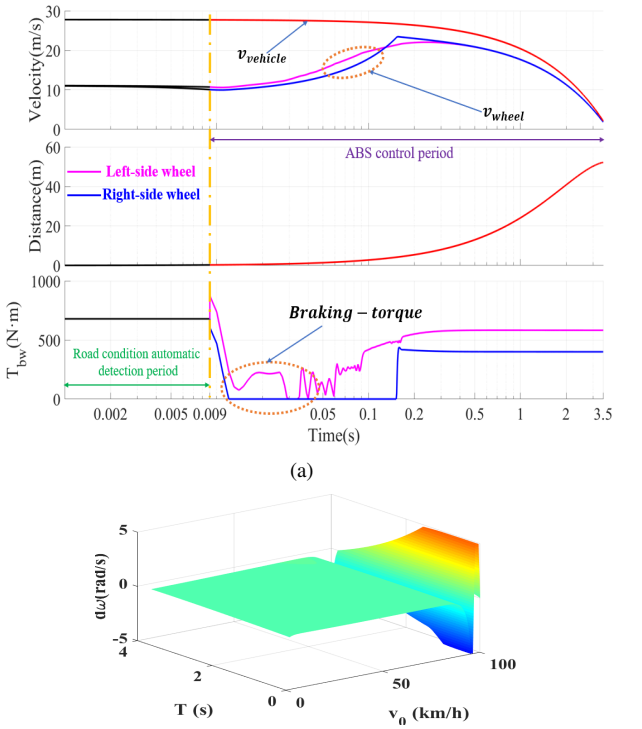

Fig. 7. Left side wheels: dry road; right side wheels: wet road: (a) regulation of braking parameters (b) trends of ω_i differential.

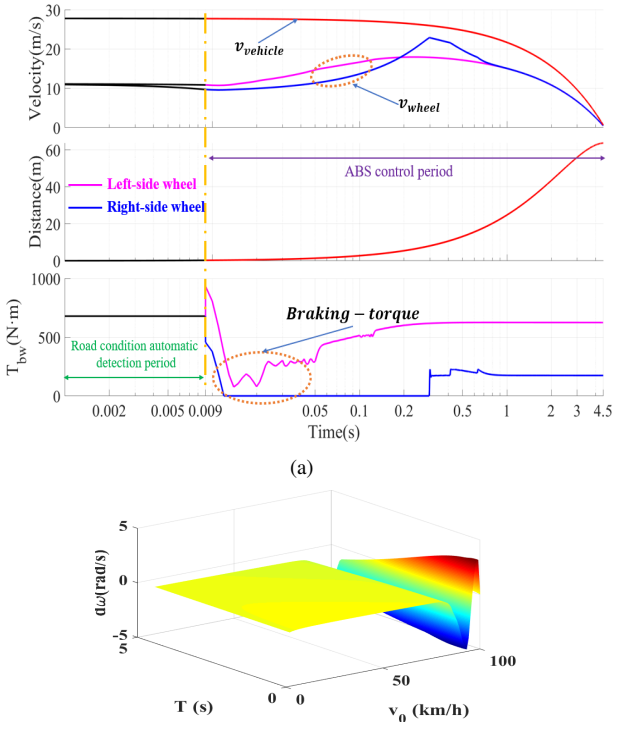

Fig. 8. Left-wheel: dry road and right-wheel: snow road: wet road: (a) regulation of braking parameters (b) trends of ω_i differential.

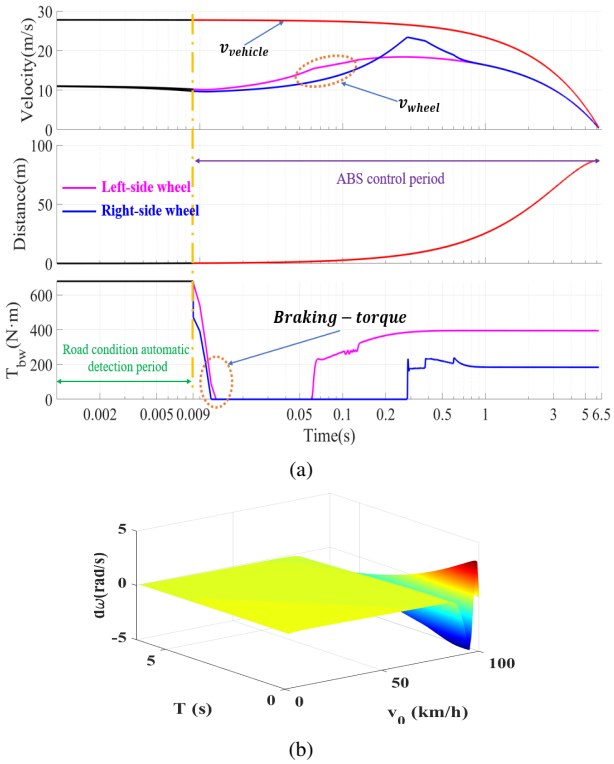

Fig. 9. Left-wheel: wet road and right-wheel: snow road: wet road: (a) regulation of braking parameters (b) trends of ω_i differential.

This split-road condition case: left side with dry road and right side with wet road is shown in Figure 7, Figure 7(b) gives the 3D regulation hook surface of $d_{\omega_{F,R}(t_k)}$. From the real-time trends of parameters shown in Figure 7(a), we can see that the vehicle braking performances under the FSM-WSC based ABS controller satisfy the safety requirement mentioned above. Thanks to the wheel smooth-braking adjustment added in the intelligent detection module, the differential between left and right wheels are always limited within a safety indicator, clearly shown in Figure 7(b).

In addition, two other split-road cases are also studied, which braking results are shown in Figure 8 and Figure 9, respectively. In the same way, the regulation details of velocities $(v_{v_x}, v_{FL}, v_{FR})$, D and T_{b_i} are reasonable. Due to the limitation on ω_i differential, considering the safety indicator, the trends of $d_{\omega_{F,R}(t_k)}$ shown in Figure 8(b) and Figure 9(b) will be restricted during whole braking period.

Despite the fact that these cases commonly exist in a real situation, an extremely complex case is also studied in this section, in which the road conditions of every single wheel are different. For example, the vehicle is braking on a dry road, whereas the dry road at different levels, that is to say, every single wheel has a different road friction coefficient, whose details are shown in Figure 10. Velocities $(v_{v_x}, v_{FL}, v_{FR}, v_{RL}, v_{RR})$, D and T_{b_i} are shown in Figure 10(a) in detail, it is clear that with the proposed brake control system, each ω_i can be quickly adjusted by T_{b_i} regulation. Moreover, the real-time road friction coefficient of each single wheel is given in Figure 10(b) intuitively. Obviously, every single wheel demonstrates different real-time $\mu_i(\lambda_i)$ regulation curve accompanying by v_{v_x} decreases.

Obviously, the proposed FSM-WSC based ABS controller and four-wheel ABS have the capability to mitigate effects that derived from the common split-road condition situations.

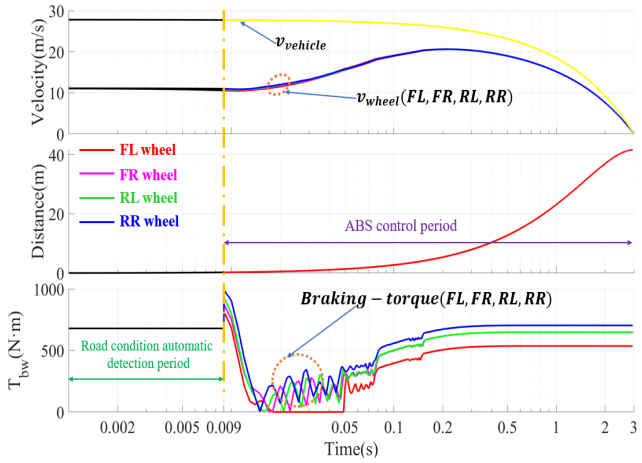

(a)

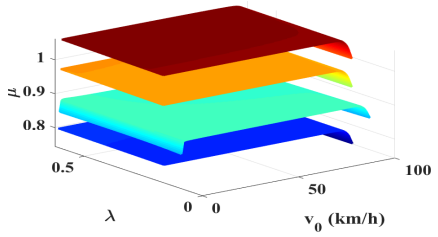

(b)

Fig. 10. Every wheel has its own road condition on dry road: (a) regulation of braking parameters (b) trends of ω_i differential.

VI. Conclusion

In this paper, the FSM-WSC based ABS controller for the four-wheel ABS is proposed, and the control performance has been verified via a variety of braking simulations under the complex road conditions mentioned above, including the transition of road conditions and the split-road conditions. Besides, the intelligent automatic detection module provides the operating basis of the second module, and the controller module provides robust and fast ABS control, which has substantial capability to deal with the complexed braking situations. In addition, the proposed four-wheel ABS has been verified by the simulated results under complex road situations has well robustness, better self-adaptation, and faster response.

References

[1] A. Dadashnialehi, A. Bab-Hadiashar, Z. Cao, and A. Kapoor, "Intelligent sensorless antilock braking system for brushless in-wheel electric vehicles," *IEEE Transactions on Industrial Electronics*, vol. 62, no. 3, pp. 1629–1638, Mar. 2015.

[2] X. D. Xue, K. W. E. Cheng, T. W. Ng, and N. C. Cheung, "Multi-objective optimization design of in-wheel switched reluctance motors in electric vehicles," *IEEE Transactions on Industrial Electronics*, vol. 57, no. 9, pp. 2980–2987, Sep. 2010.

[3] D. Savitski, D. Schleinin, V. Ivanov, and K. Augsburg, "Robust continuous wheel slip control with reference adaptation: Application to the brake system with decoupled architecture," *IEEE Transactions on Industrial Informatics*, vol. 14, no. 9, pp. 4212–4223, Sep. 2018.

[4] H. Jing, Z. Liu, and H. Chen, "A switched control strategy for antilock braking system with on/off valves," *IEEE Transactions on Vehicular Technology*, vol. 60, no. 4, pp. 1470–1484, May. 2011.

[5] J. J. Castillo, J. A. Cabrera, A. J. Guerra, and A. Simon, "A novel electrohydraulic brake system with tire road friction estimation and continuous brake pressure control," *IEEE Transactions on Industrial Electronics*, vol. 63, no. 3, pp. 1863–1875, Mar. 2016.

[6] K. Han, B. Lee, and S. B. Choi, "Development of an antilock brake system for electric vehicles without wheel slip and road friction information," *IEEE Transactions on Vehicular Technology*, vol. 68, no. 6, pp. 5506–5517, Jun. 2019.

[7] Z. Sun, J. Zheng, Z. Man, and H. Wang, "Robust control of a vehicle steer-by-wire system using adaptive sliding mode," *IEEE Transactions on Industrial Electronics*, vol. 63, no. 4, pp. 2251–2262, Apr. 2016.

[8] A. Dadashnialehi, A. Bab-Hadiashar, Z. Cao, and A. Kapoor, "Intelligent sensorless abs for in-wheel electric vehicles," *IEEE Transactions on Industrial Electronics*, vol. 61, no. 4, pp. 1957–1969, Apr. 2014.

[9] Y. Chen, C. Tu, and C. Lin, "Integrated electromagnetic braking/driving control of electric vehicles using fuzzy inference," *IET Electric Power Applications*, vol. 13, no. 7, pp. 1014–1021, 2019.

[10] D. Savitski, V. Ivanov, D. Schleinin, K. Augsburg, T. PÃ$\frac{1}{4}$tz, and C. F. Lee, "Advanced control functions of decoupled electro-hydraulic brake system," *2016 IEEE 14th International Workshop on Advanced Motion Control (AMC)*,

[11] D. Tavernini, F. Vacca, M. Metzler, D. Savitski, V. Ivanov, P. Gruber, A. E. Hartavi Karci, M. Dhaens, and A. Sorniotti, "An explicit nonlinear model predictive abs controller for electro-hydraulic braking systems," *IEEE Transactions on Industrial Electronics*, pp. 1–1, 2019.

[12] H. R. More, A. A. Digrase, and A. V. Wayse, "Linear pid control technique for single wheel abs (anti-lock braking system) of motorcycle," *2017 2nd International Conference for Convergence in Technology (I2CT)*, pp. 277–281, Apr. 2017.

[13] A. Patil, D. Ginoya, P. D. Shendge, and S. B. Phadke, "Uncertainty-estimation-based approach to antilock braking systems," *IEEE Transactions on Vehicular Technology*, vol. 65, no. 3, pp. 1171–1185, Mar. 2016.

[14] H. Sun, J. Yan, Y. Qu, and J. Ren, "Sensor fault-tolerant observer applied in uav anti-skid braking control under control input constraint," *Journal of Systems Engineering and Electronics*, vol. 28, no. 1, pp. 126–136, Feb. 2017.

[15] S. Li, J. Zhao, S. Yang, and H. Fan, "Research on a coordinated cornering brake control of three-axle heavy vehicles based on hardware-in-loop test," *IET Intelligent Transport Systems*, vol. 13, no. 5, pp. 905–914, 2019.

[16] V. Ivanov, D. Savitski, and B. Shyrokau, "A survey of traction control and antilock braking systems of full electric vehicles with individually controlled electric motors," *IEEE Transactions on Vehicular Technology*, vol. 64, no. 9, pp. 3878–3896, Sep. 2015.

[17] W. Sun, J. Zhang, and Z. Liu, "Two-time-scale redesign for antilock braking systems of ground vehicles," *IEEE Transactions on Industrial Electronics*, vol. 66, no. 6, pp. 4577–4586, Jun. 2019.

[18] A. Dadashnialehi, A. Bab-Hadiashar, Z. Cao, and R. Hoseinnezhad, "Reliable emf-sensor-fusion-based antilock braking system for bldc motor in-wheel electric vehicles," *IEEE Sensors Letters*, vol. 1, no. 3, pp. 1–4, Jun. 2017.

[19] Z. Wei and G. Xuexun, "An abs control strategy for commercial vehicle," *IEEE/ASME Transactions on Mechatronics*, vol. 20, no. 1, pp. 384–392, Feb. 2015.

[20] Y. Wang, H. Fujimoto, and S. Hara, "Driving force distribution and control for ev with four in-wheel motors: A case study of acceleration on split-friction surfaces," *IEEE Transactions on Industrial Electronics*, vol. 64, no. 4, pp. 3380–3388, Apr. 2017.

[21] X. Wu, M. Zhang, and M. Xu, "Active tracking control for steer-by-wire system with disturbance observer," *IEEE Transactions on Vehicular Technology*, vol. 68, no. 6, pp. 5483–5493, Jun. 2019.

[22] J. Ni, J. Hu, and C. Xiang, "Envelope control for four-wheel independently actuated autonomous ground vehicle through afs/dyc integrated control," *IEEE Transactions on Vehicular Technology*, vol. 66, no. 11, pp. 9712–9726, Nov. 2017.

[23] H. Yu, F. Cheli, and F. Castelli-Dezza, "Optimal design and control of 4-iwd electric vehicles based on a 14-dof vehicle model," *IEEE Transactions on Vehicular Technology*, vol. 67, no. 11, pp. 10 457–10 469, Nov. 2018.

[24] J. Sun, X. Xue, and K. Cheng, "Fuzzy sliding mode wheel slip ratio control for smart vehicle anti-lock braking system," *Energies*, vol. 12, no. 13, pp. 2501, Jun. 2019.